*Master's Thesis in Photonics Engineering*

# Fiber Optic Current Sensors

Kristian Björk Svensson


CHALMERS

SP Sveriges Tekniska Forskningsinstitut
Brinellgatan 4

Department of Microtechnology and Nanoscience
Photonics Laboratory
CHALMERS UNIVERSITY OF TECHNOLOGY
Gothenburg, Sweden 2014

Fiber Optic Current Sensors

Kristian Björk Svensson

Photonics Laboratory
Department of Microtechnology and Nanoscience
Chalmers University of Technology
SE-412 96 Göteborg
Sweden
Telephone:+46 (0)31-772 10 00

Printed in Sweden by Reproservice, Chalmers Tekniska Högskola, 2014

**Abstract**

Fiber optic current sensors utilize the Faraday effect which causes the polarization of the light to rotate. These sensors have several advantages compared to conventional current measurement methods such as electrical insulation and small size and weight. There is however requirement on specially manufactured fiber and components in order to cancel out undesired linear birefringence which will transform the polarization.

In this thesis the foundations of these system have been investigated and tested in a configuration including a SMF (Single Mode Fiber) as the sensing coil terminated with a Faraday mirror. The wavelength of operation is around 1550 nm and the number of loops in the sensing coil is approximately 2100. The SMF was not preferable in these types of sensors and it is recommended to use spun highly birefringent fiber for such large number of loops in order to cancel out the linear birefringence properly.

**Acknowledgements**

I am would like thank for the opportunity to work and learn about this new field within the area of current measurements. I would like thank my supervisor Alf-Peter Elg at SP who have guided me and given me alot of useful thoughts and ideas. I would also like to thank my supervisor Pontus Johannisson at the Photonics laboratory for helping me with all fiber related problems and putting together this report. Finally, a thank to Carl Lundström at the Photonics laboratory for all assistance and instructions in the lab.

Kristian Björk Svensson, 2014

# Contents

# List of Figures

# Chapter 1

# Introduction

In today's complex electrical power distribution systems, sensors are installed to monitor currents and voltages. These will enable the capability of detecting failure in the system and prevent damages. When the electrical power distribution systems were developed in the late 19th century there was a battle between Tesla and Edison, today known as the "The battle of the currents", whether alternating current (AC) or direct current (DC) was the best alternative [1]. AC was the dominant choice since it was relatively easy to transform between different voltage levels whereas DC was almost impossible to transform at that time. Due to recent research HVDC, high voltage direct current, has lately become popular for electrical power transmission since it does notsuffer as much from losses during transmission as AC [1]. It is also cheaper, has greater energy efficiency and the equiment is smaller. In order to measure current there are several different techniques, slightly different depending on if it is AC or DC, but one newly developed technique that is applicable on both AC and DC is the fiber-optic current sensor [2], which is based on the magneto-optic Faraday effect. The Faraday effect causes the polarization of a lightwave to rotate due to a longitudinal magnetic field. Basically, a polarized wave is lunched into a sensing fiber wound around the conductor of interest. The wave returns and a receiver detects the Faraday phase shift and can then determine the magnitude of the current. There are several advantages for this sensor compared to conventional current sensors, including electric isolation due to the non-electric nature of optical fibers [2]–[5]. These sensors are also small in size and weight [4]–[6]. This will allow the possibility of installing these sensors on existing high-voltage components. Furthermore, these sensors will not suffer from ferromagnetic resonance or magnetic saturation. Also there will be no risk of catastrophic event such as explosion which may occur with conventional instruments with oil insulation [5, 6]. In addition, these sensors have high bandwidth [6] which enable pos-

sibility to detect the occurence of high frequency transients. However, there are also non-desirable effects in the fiber optic current sensor that will require cancellation in order to keep the sensor sensitive to the Faraday effect. Since the state of polarization is the information carrier, high quality fiber with low linear birefringence needs to be used since linear birefringence will result in polarization transformation which in turn will decrease the sensitivity of the sensor. It should also be noted that compared to linear birefringence the Faraday effect is often weak and may be masked which will complicate the measurement of the rotation [7].

This report will give some background of polarization and polarization effects in chapter 2 and 3. In chapter 4, different configurations for detecting the Faraday effect will be described and also pinpoint where the crucial parts of the sensor are. Some result from previous work will also be discussed in chapter 4. This work also include some current measurements using a simple setup which is described in chapter 5 and the results from these measurements are presented in chapter 6 with discussion. Finally, conclusion and additional discussion is presented in chapter 7.

# Chapter 2

# Light and polarization

Light is electromagnetic radiation and consists of both an electric field and a magnetic field. The polarization of a given wave is determined by the electrical field. Light can either be linearly, elliptically, circularly or randomlypolarized. In this chapter some background to light and polarization will be presented. There will also be a brief discussion on how different states of polarization can be illustrated and described mathematically.

## 2.1 Linear polarization

A linearly polarized wave has an electric field vector contained within a plane along the path of propagation. This wave can be decomposed into two mutually orthogonal components along the x- and y-direction, respectively. These components can be expressed as

$$\mathbf{E}_x(z,t) = \hat{x}E_{x0}\cos(kz - \omega t) \tag{2.1}$$

and

$$\mathbf{E}_y(z,t) = \hat{y}E_{y0}\cos(kz - \omega t + \phi) \tag{2.2}$$

where $\phi$ is the relative phase difference between the two components. If $\phi = \pm\pi n$, where $n$ is an integer, a wave described by the equations above is linearly polarized [8]. If $\phi = \pm 2\pi n$ then the two wave components are in-phase and the resulting wave can be described as

$$\mathbf{E}(z,t) = \mathbf{E}_x(z,t) + \mathbf{E}_y(z,t) = (\hat{x}E_{x0} + \hat{y}E_{y0})\cos(kz - \omega t). \tag{2.3}$$

If $\phi = \pm\pi n$, where $n$ is an odd integer, then the two components are 180° out of phase and the resulting wave can be described as

$$\mathbf{E} = (\hat{x}E_{x0} - \hat{y}E_{y0})\cos(kz - \omega t) \tag{2.4}$$

A wave described by Eq. 2.4 is also linearly polarized but the plane of polarization is rotated compared to the previous case.

## 2.2 Circular polarization

In the previous section the relative phase difference between the two orthogonal x- and y-component was multiples of $\pi$. If the relative phase difference $\phi = -\pi/2 + 2m\pi$, where $m = 0, \pm 1, \pm 2, \ldots$, and the amplitudes are equal ($E_{x0} = E_{y0} = E_0$) the polarization will be circular. This means that at any fixed point along the path of propagation the electrical field vector will rotate around the z-axis. A wave with a circular polarization can be expressed with the components

$$\mathbf{E}_x(z,t) = \hat{x} E_{x0} \cos(kz - \omega t) \tag{2.5}$$

and

$$\mathbf{E}_y(z,t) = \hat{y} E_{y0} \sin(kz - \omega t) \tag{2.6}$$

The resulting wave is then expressed as

$$\mathbf{E} = E_0 \left[\hat{x} \cos(kz - \omega t) + \hat{y} \sin(kz - \omega t)\right]. \tag{2.7}$$

A circularly polarized wave described by Eq. 2.7 is referred to as right-hand circular polarized and rotates counterclockwise when travelling towards an observer.

If the relative phase difference is $\phi = \pi/2 + 2m\pi$, where $m = 0, \pm 1, \pm 2, \ldots$, the resulting wave can be expressed as

$$\mathbf{E} = E_0 \left[\hat{x} \cos(kz - \omega t) - \hat{y} \sin(kz - \omega t)\right], \tag{2.8}$$

and the wave have left-hand circular polarization and is rotating clockwise when travelling towards an observer.

Both linear polarization and circular polarization can be considered as special cases of elliptical polarization. Elliptical polarization means that the electric field vector is rotating and has different amplitudes in x- and y-directions.

## 2.3 Stokes parameters and the Jones vectors

A convenient way of expressing polarized light is by using Jones vectors,

$$\vec{E} = \begin{pmatrix} E_x \\ E_y \end{pmatrix} = \begin{pmatrix} E_{0x}e^{j\phi_x} \\ E_{0y}e^{j\phi_y} \end{pmatrix} \tag{2.9}$$

here represented by using complex phasors. One drawback with Jones vectors is that it can only be used on polarized waves [8]. Another way of expressing light waves is by using Stokes parameters and combine them into a Stokes vector [9]. Using Jones vector components the Stokes vector can be expressed as

$$\vec{S} = \begin{pmatrix} S_0 \\ S_1 \\ S_2 \\ S_3 \end{pmatrix} = \begin{pmatrix} |E_x|^2 + |E_y|^2 \\ |E_x|^2 - |E_y|^2 \\ E_x^* E_y + E_x E_y^* \\ -jE_x^* E_y + jE_x E_y^* \end{pmatrix} \tag{2.10}$$

where the first parameter, $S_0$, represents the total power of the light. $S_1$ represents if the wave hasmore tendency to resemble horizontal polarization ($S_1 > 0$) or vertical polarization ($S_1 < 0$), $S_2$ represents if the wave has more tendency to resemble $45°$ polarization ($S_2 > 0$) or $-45°$ polarization ($S_2 < 0$) and $S_3$ represents if the wave has more tendency to resemble right-handedness ($S_3 > 0$) or left-handedness ($S_3 < 0$). In the case of fully polarized light $S_0^2 = S_1^2 + S_2^2 + S_3^2$ and in the other extreme, unpolarized light, $S_1 = S_2 = S_3 = 0$. Examples of Stokes and Jones vectors of different polarizations are shown i Table 2.1. Since all light is polarized instantaneously, it is preferable to express these parameters in time averages in order to distinguish between polarized and unpolarized light.

The Stokes parameters $S_1, S_2, S_3$ form a 3D-space referred to as the Stokes space. These three parameters forms a sphere referred to as the Poincaré sphere, shown in Fig. 2.1.

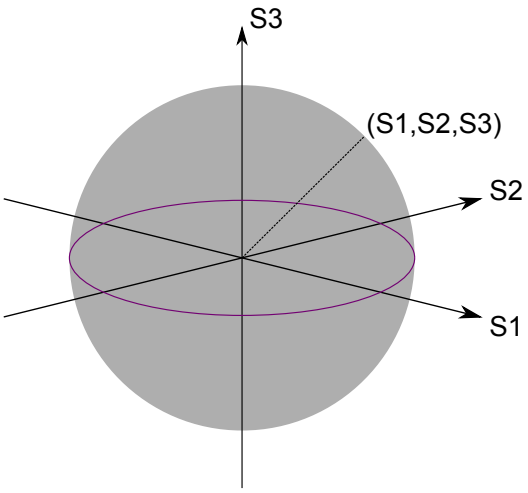


Figure 2.1: A schematic of the Poincaré sphere in the Stokes space. At the equator the polarization is linear, at the poles the polarization is circular and in between the polarization is elliptical.

The polarization can also be described in terms of axes of the polarization ellipse, the orientation of the ellipse and the sense of rotation, see Fig. 2.2. This is a convenient approach since the Stokes parameters corresponds to measurable intensities [10]. The Stokes parameters, in terms of the parameters of the polarization ellipse are

$$\begin{pmatrix} S_0 \\ S_1 \\ S_2 \\ S_3 \end{pmatrix} = \begin{pmatrix} A^2 + B^2 \\ (A^2 - B^2)\cos(2\theta) \\ (A^2 - B^2)\sin(2\theta) \\ 2ABh \end{pmatrix} \tag{2.11}$$

where $A$ and $B$ are the semi-major and the semi-minor axis, respectively, of the ellipse, $\theta$ is the angle between the semi-major axis and the x-axis and $h$ is the sense of rotation.

| State of polarization | Jones vectors | Stokes vectors |
|---|---|---|
| Linear vertical polarization | $\begin{pmatrix} 0 \\ 1 \end{pmatrix}$ | $\begin{pmatrix} 1 \\ -1 \\ 0 \\ 0 \end{pmatrix}$ |
| Linear horizontal polarization | $\begin{pmatrix} 1 \\ 0 \end{pmatrix}$ | $\begin{pmatrix} 1 \\ 1 \\ 0 \\ 0 \end{pmatrix}$ |
| Linear polarization at $-45°$ | $\frac{1}{\sqrt{2}}\begin{pmatrix} 1 \\ -1 \end{pmatrix}$ | $\begin{pmatrix} 1 \\ 0 \\ -1 \\ 0 \end{pmatrix}$ |
| Linear polarization at $45°$ | $\frac{1}{\sqrt{2}}\begin{pmatrix} 1 \\ 1 \end{pmatrix}$ | $\begin{pmatrix} 1 \\ 0 \\ 1 \\ 0 \end{pmatrix}$ |
| Left-hand circular polarization | $\frac{1}{\sqrt{2}}\begin{pmatrix} 1 \\ i \end{pmatrix}$ | $\begin{pmatrix} 1 \\ 0 \\ 0 \\ -1 \end{pmatrix}$ |
| Right-hand circular polarization | $\frac{1}{\sqrt{2}}\begin{pmatrix} 1 \\ -i \end{pmatrix}$ | $\begin{pmatrix} 1 \\ 0 \\ 0 \\ 1 \end{pmatrix}$ |

Table 2.1: Examples of Stokes and Jones vectors for different polarizations [8].

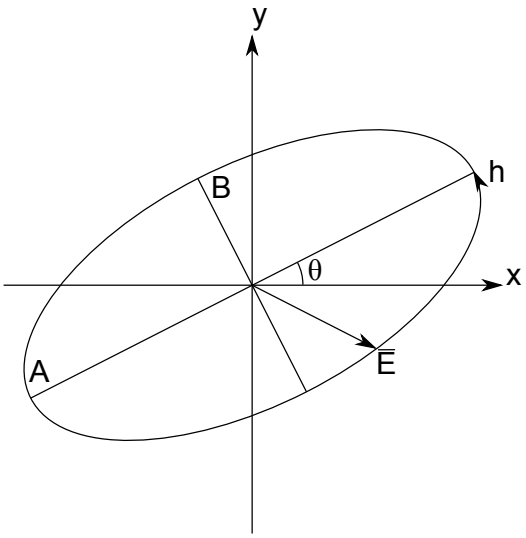


Figure 2.2: A schematic of the polarization ellipse. $A$ and $B$ are the semi-major and semi-minor axes of the ellipse, respectively, and h is the sense of rotation.

# Chapter 3

# Polarization effects in optical fibers

In this chapter background theory and the origin of both birefringence and the Faraday effect will be presented.

## 3.1 Birefringence in fibers

One very important issue in optical fibers is the presence of birefringence, which can result in change of the state of polarization. In the field of optical sensors, unstable polarization or drift of polarization is not desirable due to the fact that the state of polarization is the information carrier. Birefringence will create distortion and the sensitivity of the sensor will decrease.

There are two types of birefringence: linear and circular birefringence. These can either be inherent or induced [11]. In SMF (single-mode fiber) both inherent and induced linear birefringence needs to be considered whereas inherent circular birefringence often can be neglected.

### 3.1.1 Linear birefringence

Consider a linearly polarized wave, with an electrical field intensity vector **E**, travelling in the z-direction. As mentioned in section 2.1, the wave can be decomposed into $E_x$ and $E_y$ components i x- and y-direction, respectively. In an ideal fiber, with a circular cross-section and homogeneous composition of materials, the wave number for the two orthogonal components will be the same. However, if there is a slight deviation from homogeneous circular cross-section, i.e. elliptical cross-section or inhomogeneous material, the refractive index will not be the same for the two components which will result

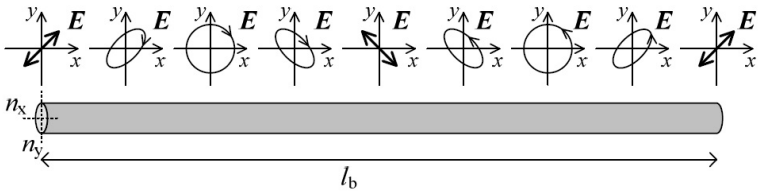


Figure 3.1: Illustration of polarization transformation due to linear birefringence along a fiber [11]. $l_B$ is the beat length.

in different wave numbers for $E_x$ and $E_y$. The two components will travel at different velocities, resulting in a relative phase shift between them. The linearly polarized wave will become elliptical and later circular. Then it will be transformed back to linear polarization, passing through a state of elliptical polarization. This linear state of polarization is orthogonal to the original linear polarization. The polarization will change as before one more time, with opposite handedness as before, and finally the polarization is back to the original one. At this point, the phase shift is $2\pi$ and the fiber length the wave has to travel in order to reach the original polarization is defined as the beat length. This polarization transformation is shown in Fig. 3.1.
The beat length is given by

$$l_b = \frac{\lambda}{n_{x,\text{eff}} - n_{y,\text{eff}}} = \frac{\lambda}{\Delta n_{\text{eff}}} \tag{3.1}$$

where $n_{\text{x,eff}}$ and $n_{\text{y,eff}}$ are the effective refractive indices in x- and y-direction, respectively, and $\lambda$ is the wavelength.

As mentioned before, fiber with elliptical core cross-section is a source of linear birefringence. When manufacturing optical fibers ideal circular core cross-section is hard to achieve and the core cross-section will be slightly elliptical. This is the main source of inherent linear birefringence. Common fibers with an output polarization state close to the input polarization state are just a few meters long [11].

Another source of linear birefringence imposed during the manufacturing process is inner mechanical stress on the core [11]. Non-homogeneous density of the cladding will causes stress on the core which results in birefringence.

Linear birefringence is not only caused by imperfections during the manufacturing, but can be induced by external influence. One considerable source is the bending of fibers, which is especially an important consideration in fiber optic current sensor since the fiber is wound around a current conductor. When bending a fiber mechanical stress will be imposed on the cladding which is transfered into the core and results in linear birefringence.

### 3.1.2 Circular birefringence

Circular birefringence is similar to linear birefringence, but instead of exhibiting refractive indices $n_x$ and $n_y$ in x- and y-direction, respectively, the wave exhibits refractive indices $n_r$ and $n_l$ for right-hand circular polarization and left-hand circular polarization, respectively. As mentioned before, inherent circular birefringence of single mode fiber is negligible in contrast to inherent linear birefringence. However, circular birefringence can be imposed during manufacturing by spinning the fiber during the fiber drawing process [11, 12]. Circular birefringence can also be induced in the fiber after manufacturing by twisting it.

## 3.2 Magneto-optical effect

It is not only mechanical stress applied upon the fiber that can cause birefringence, it can also origin from magneto-optical effects. There are several types of magneto-optical effect [8, 13, 14]:

- The Faraday effect
- The Cotton-Mouton effect
- The Voigt effect

The Faraday effect, sometime referred to as Faraday rotation, is based on interaction between the external magnetic field and the oscillation of the electrons in the medium. Assume that a linearly polarized wave, which can be considered as superposition of one left-hand circularly polarized wave and one right-hand circularly polarized wave, enters a medium. Circularly polarized light will cause the electrons to rotate around their respective nucleus and the charge polarization will be proportional to the radius of this circle [8]. In the case of a longitudinal magnetic field within the medium there will be a radially directed force $\mathbf{F} = q\mathbf{v} \times \mathbf{B}$ on the electron. Hence, the radius will change. If the direction of the rotation is reversed, the sign will change of the radial force. The charge polarization is related to the electric field of the wave via the susceptibility and it can be concluded that the susceptibility is different for right-hand and left-hand circularly polarization. The refractive index depends on the susceptibility and hence the two circular components will propagate with different velocities. This will result in a linear polarization slightly rotated at the output of the medium compared with the polarization at the input. An illustration of the Faraday effect is shown in Fig. 3.2. Using Jones calculus this can be shown matematically.

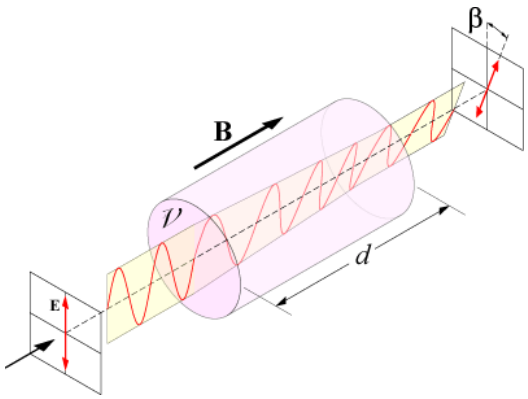


Figure 3.2: Faraday effect on a linearly polarized wave entering a medium of length $d$ and with a magnetic flux density of $\mathbf{B}$ [15].

Starting with the Jones matrix for a counterclockwise rotation of the plane of polarizations

$$\mathbf{T}_F = \begin{pmatrix} \cos\theta_F & -\sin\theta_F \\ \sin\theta_F & \cos\theta_F \end{pmatrix} \tag{3.2}$$

and assuming that light with a horisontal linear polarization is rotated 90°, that is

$$\begin{pmatrix} 0 & -1 \\ 1 & 0 \end{pmatrix} \begin{pmatrix} 1 \\ 0 \end{pmatrix} = \begin{pmatrix} 0 \\ 1 \end{pmatrix} \tag{3.3}$$

This is consistent with the Jones vector for linear y-polarization which is shown in Table 2.1. Continuing with seeing a horisontal linear polarization as superposition of two circular polarization with opposite rotation

$$\begin{pmatrix} 1 \\ 0 \end{pmatrix} = \frac{1}{2}\begin{pmatrix} 1 \\ i \end{pmatrix} + \frac{1}{2}\begin{pmatrix} 1 \\ -i \end{pmatrix} \tag{3.4}$$

and letting $\mathbf{T}_F$ operate on each polarization seperately. This will result in

$$\mathbf{T}_F \frac{1}{2}\begin{pmatrix} 1 \\ i \end{pmatrix} = \frac{1}{2}\begin{pmatrix} \cos\theta_F - i\sin\theta_F \\ \sin\theta_F + i\cos\theta_F \end{pmatrix} = \frac{1}{2}\begin{pmatrix} e^{-i\theta_F} \\ ie^{-\theta_F} \end{pmatrix} = e^{-i\theta_F}\frac{1}{2}\begin{pmatrix} 1 \\ i \end{pmatrix} \tag{3.5}$$

and

$$\mathbf{T}_F \frac{1}{2}\begin{pmatrix} 1 \\ -i \end{pmatrix} = \frac{1}{2}\begin{pmatrix} \cos\theta_F + i\sin\theta_F \\ \sin\theta_F - i\cos\theta_F \end{pmatrix} = \frac{1}{2}\begin{pmatrix} e^{i\theta_F} \\ -ie^{\theta_F} \end{pmatrix} = e^{i\theta_F}\frac{1}{2}\begin{pmatrix} 1 \\ -i \end{pmatrix} \tag{3.6}$$

and it can be concluded that the phase shift is identical but with different signs for the two polarization states.

The resulting rotation of the polarization is found to be [7]

$$\phi_F = V \int \mathbf{B} \cdot d\mathbf{l} \tag{3.7}$$

where $\theta_\mathrm{F}$ is the angle of rotation (rad) caused by the Faraday effect, $V$ is the Verdet constant ($\mathrm{rad} \cdot \mathrm{T}^{-1} \cdot \mathrm{m}^{-1}$) and $\mathbf{B}$ is the magnetic flux density (T or $\mathrm{Wb} \cdot \mathrm{m}^{-2}$). Equation (3.7) holds under the assumption that the Verdet constant is unchanged along the path. If the Verdet constant is spatially dependent the Verdet constant must be included in the integration.

In current sensor applications the fiber often encloses the current carrying-conductor with an integer number of loops. Using this fact Ampère's law can then be applied and simplify Eq. 3.7 to

$$\phi_F = VNI \tag{3.8}$$

where $N$ is the number of loops around the conductor and $I$ is the current flowing through the conductor. The Faraday effect is non-reciprocal and hence the direction of the polarization rotation depends both on the direction of the wave propagation and the direction of the magnetic field. If the wave travels in opposite direction relative to the magnetic field, the rotation will be in opposite direction compared to the case when the wave travelled along the same direction as the magnetic field. If two waves propagate along a magnetic field, one right-hand circularly polarized wave and one left-hand circularly polarized wave, one of them will experience a positive phase shift whereas the other will experience a negative phase shift. In other words, they will experience a relative phase shift two times the Faraday effect. Finally, if two waves propagate in different directions and with different handedness on the polarization, they will experience the same phase shift.

Compared to the Voigt effect, which is a result of a transverse magnetic field [13], the Faraday effect is orders of magnitudes larger in optical fibers. This is because the phase shift resulting from the Voigt effect is quadratic dependent on the transverse magnetic field,

$$\phi_V = V_q \int \mathbf{H}_T^2 \cdot d\mathbf{l} \tag{3.9}$$

where $V_q$ is the Voigt constant and is given by

$$V_q = \frac{n\lambda}{\pi(n^2 - 1)} V^2 \tag{3.10}$$

and rules out the Voigt effect for current sensing applications in most cases.

The third magneto-optical effect, the Cotton-Mouton effect, is the same as the Voigt effect in a phonomenological point of view but the has values of $V_q$ much larger. However, it is still too small for current sensing applications [13].

## 3.3 Verdet constant

The Verdet constant is a measure of how strong the Faraday effect is in a particular material. The Verdet constant is also wavelength dependent and will be affected by temperature. In order to keep high sensitivity for the sensor a stable Verdet constant is required which in turn will put certain requirement on both the material and the wavelength of operation.

### 3.3.1 Wavelength dependence of the Verdet constant

The Verdet constant is inversely proportional to the wavelength squared, $1/\lambda^2$ [6]. A 20 nm change in wavelength will then result in 5 % change in sensitivity [16]. For silica fiber, the Verdet constant is given by the following formula

$$V = 0.142 \cdot 10^{-28} \cdot \nu^2 \tag{3.11}$$

with the unit rad $\cdot$ T$^{-1}$ $\cdot$ m$^{-1}$ and where $\nu$ is the frequency in Hz. This clearly shows that in order to achieve higher sensitivity in the sensor lower wavelength is desirable. In current sensing application it may be more preferable to use the unit rad A$^{-1}$. The Verdet constant for silica is plotted in Fig 3.11.

### 3.3.2 Temperature dependence of the Verdet constant

There are always requirements on accuracy when doing measurements. Furthermore, there also may be requirements of keeping the accuracy even if the temperature is changing. In electrical substations, sensors needs to keep an accuracy of $\pm 0.2\%$ [3] with temperature ranging from $-40$°C to 85°C. Fiber optic current sensors have in the past experienced high sensitivity to temperature, which have limited the performance severely. The main reason for this is that temperature changes result in stress-induced linear birefringence in the sensing coil of the sensor [3]. Even though several techniques have been proposed in order to increase the performance, there is still the matter of the inherent temperature dependence of the Verdet constant, which is $0.7 \cdot 10^{-4}$ °C$^{-1}$ for fused silica [17].

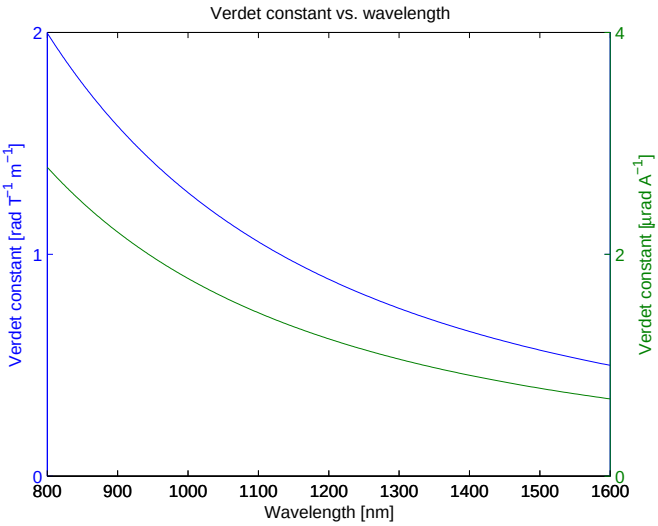


(a) Verdet constant for silica from 800 nm up to 1600 nm.

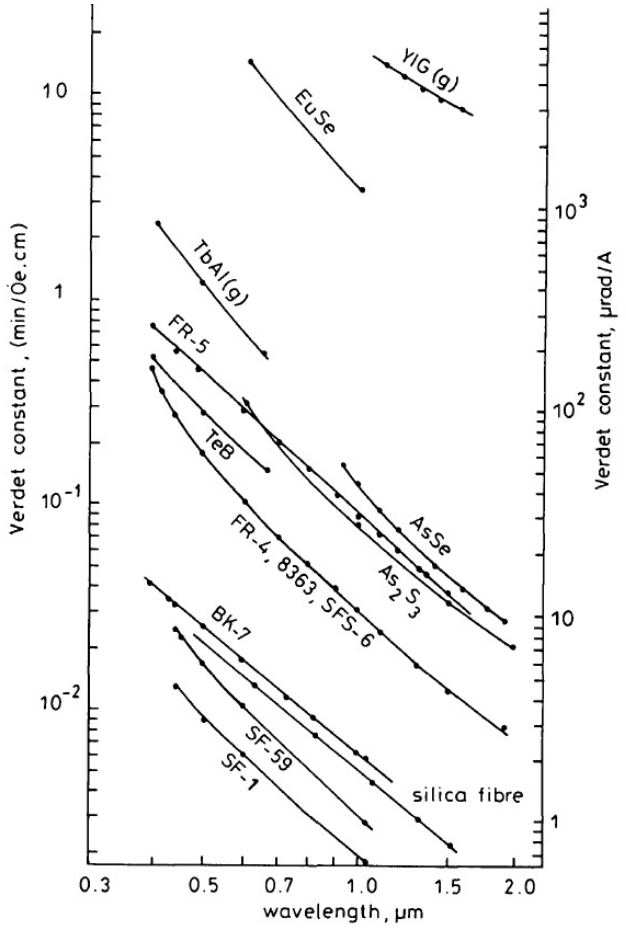


(b) Verdet constant for different materials [13].

Figure 3.3

# Chapter 4

# Sensor configurations and components

Several different configurations have been proposed in order to detect the Faraday effect, where the two most common are the Sagnac configuration and the reflection configuration. In this chapter these two configurations will be described as well as the components in these configurations.

## 4.1 Reflection configuration

In the reflection configuration, also know as in-line configuration [3], the light is reflected back at the end of a sensing coil and travels back along the same path. The setup is shown in Fig. 4.1. Partially polarized light is launched from a source, passes through a coupler, and then enters a fiber polarizer to achieve completely polarized light. Because of the 45° splice between the axis of the fiber polarizer and the axis of the polarization-maintaining (PM) fiber, the wave is equally split between the x- and y-axis of the PM fiber. The phase modulator will modulate the phase difference between these two linearly polarized components. Before entering the sensing coil, the wave passes through a quarter-wave phase retarder. Because of 45° splice just before the retarder, both of the linear orthogonal components will give rise to one circularly polarization component each but with different sense of rotation. At the end of the sensing coil the wave is reflected and the two components swap positions, i.e. the one component that is right-hand circular will become left-hand circular and vice versa. Upon passing the phase retarder in the backward direction, the circular components are converted back to linear components. Due to the fact that the two components swapped positions when they were reflected the linear components are interchanged, i.e. the

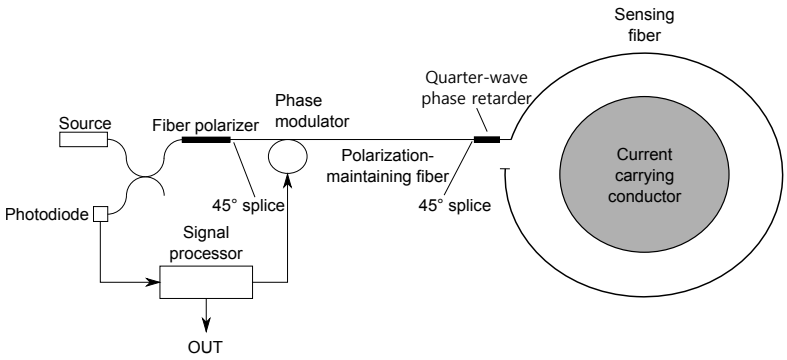


Figure 4.1: A schematic drawing of the setup of the reflection configuration [3].

one component parallell to the x-axis at the input will be parallell to the y-axis at the output and vice versa. The PM fibers will induce a relative phase different between the two components since there is one fast axis and one slow axis but since the components are swapped the relative phase difference will become zero after the backward propagation.

If there is a current present in the conductor, i.e. there is a magnetic field around the conductor, there will be an induced phase shift between the two components that is four times the Faraday phase shift [3, 5, 18]

$$\Delta\phi_R = 4\phi_F \tag{4.1}$$

The reason that the observed phase shift is four times the Faraday phase shift is due to the fact of the non-reciprocity nature of the Faraday effect. Since the wave is transformed into one right-hand circular component and one left-hand circular component, there will be a relative phase shift two times the Faraday phase shift after the forward pass through the sensing coil. On the way back, with swapped polarization, the wave will once again experience a phase shift that is two times the Faraday phase shift and the total phase shift will result in four times the Faraday phase shift. One big advantage with this type of configuration compared to the Sagnac configuration, which will be discussed in the next section, is that it is more tolerable against vibrations, about up to 1000 times less sensitive to disturbance than the Sagnac configuration [3].

Frosio and Dändliker [2] performed very comprehensive theoretical analysis on this configuration. They also performed measurements to compare different types of sources and measurements to see the effect of nonreciprocal phase shift induced by the phase modulator. Without nonreciprocal phase shift the sensor had good linearity on 75 Hz ac current ranging from 0 A to

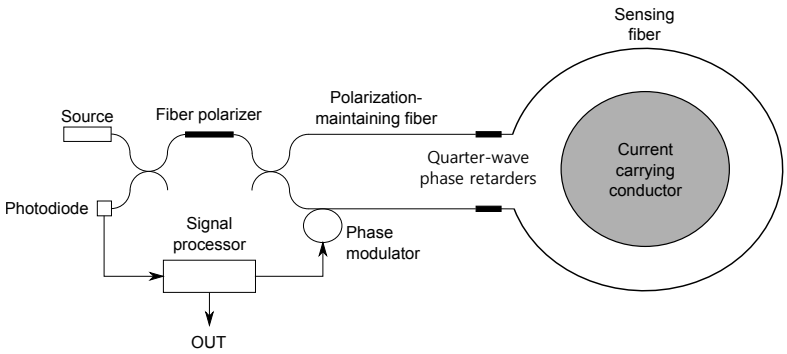


Figure 4.2: A schematic drawing of the setup of the Sagnac configuration [3].

40 A and the measured noise was 70 times higher than the calculated shot noise limit for that level of optical power. With nonreciprocal phase shift Frosio and Dändliker managed to achieve a noise level that was 20 times higher than the calculated shot noise limit. From the measurement with different sources they concluded that a low coherence source ( $200\mu m$) could be able to eliminate pertubations resulting from polarization cross coupling. A 100-turn sensing coil was used in their work.

Bohnert et.al. [3] were mainly focused on the effect on temperature dependence and sensitivity to mechanical vibration on both a reflection and Sagnac configuration. They performed both theoretical and experimental work on how temperature will affect the retardation in the phase retarder, how it will affect the sensitivity of the sensor and how this temperature dependence can be utilized in order to compensate for the temperature dependence of the Verdet constant. The vibration measurements subjected the sensing coils for both configurations with vibrations corresponding to $10g$ with a frequency of 50 Hz and concluded that the reflection configuration was almost immune to the vibrations with less than 0.2 rms A/$\sqrt{\text{Hz}}$ shot noise equivalent current.

## 4.2 Sagnac configuration

In the Sagnac configuration there are two counterpropagating waves that is circularly polarized and have the same handedness [2]. Compared to the reflection configuration the Sagnac configuration has two branches after the fiber polarizer. The polarizations in the different branches are parallell to each other and thus result in circularly polarizations with the same sense of rotation at the quarter wave phase retarders. After propagating around the current conductor the circular polarizations are converted back to linear polarizations. The induced phase shift between the two waves is two times

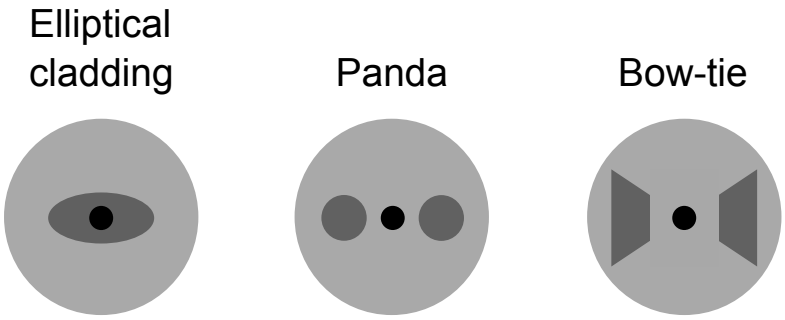


Figure 4.3: Cross-section of three types of PM fibers.

the Faraday phase shift [3, 18]

$$\Delta\phi_S = 2\phi_F \tag{4.2}$$

because of the fact that both polarizations have the same handedness and since they are propagating in different directions the resulting phase shift will be two times the Faraday phase shift. One advantage with the Sagnac configuration is that it is the same configuration used in fiber gyroscopes, hence it can be applicable without any changes [13, 16].

## 4.3 Components

### 4.3.1 Polarization-maintaining fiber

For transportation of the optical signal between the source and the sensing coil these systems utilize polarization-maintaining (PM) fibers. Using standard fiber for this could lead to distortion and transformation of the polarization state which will decrease the sensitivity of the sensor. There are several types of PM fiber:

- Elliptical cladding fiber
- Panda fiber
- Bow-tie fiber

The Elliptical cladding fiber have a cladding which is elliptical which causes an asymmetric cross-section of the fiber. The other two, Panda and Bow-tie, have rods of other material within the cladding, resulting in stress-induced linear birefringence. The cross-section of these types of fibers are shown in Fig. 4.3.

### 4.3.2 Quarter-wave phase retarder

As mentioned before, the quarter-wave phase retarder converts a linearly polarized wave into a circularly polarized wave and vice versa. A quarter-wave phase retarder has one fast axis and one slow axis, introducing a 90° phase shift between two orthogonal components of a wave [8]. If a wave is parallel to either the slow or the fast axis of the retarder the wave will be unaffected since in order to achieve a phase difference two components of the wave needs to be present. If a linear polarized wave has 45° angle to one of the axis of the retarder the phase difference between the two components will be 90° and circular polarization after the retarder will be achieved. This explains the 45° splice between the PM fibers and the phase retarder in Fig. 4.1.
One way to design a quarter-wave phase retarder for fiber optic current sensors is to fuse the polarization-maintaining fiber, which has an elliptical core, and the sensing coil together [5]. Then a 45° twist is applied over the splice, and then heated in order to soften the fiber, relaxing the twist. This then results in a quarter wave retarder region with the desired 45° offset of the core orientation with respect to the elliptical-core fiber. The procedure is shown in Fig. 4.4. One advantage with these elliptical-core fiber retarders is that the change of retardation with temperature is relatively small. Furthermore, by setting the phase retarder to 100.4° instead of 90° at room temperature this component can compensate for the temperature dependence of the Verdet constant. Bohnert et. al. [5] found that in order to keep the sensor within ±0.2° in the temperature range −40° – 85° C the retardation should be between 98.4° and 102.2° at room temperature.

### 4.3.3 Sensing coil

The heart of the fiber optic current sensor is the sensing coil, where the Faraday effect is introduced. Recall Eq. 3.7, the resulting Faraday phase shift depends on the length of the interaction between light and magnetic field. In the case of enclosure of an electric conductor with $N$ number of loops, where $N$ is an integer, Eq. 3.7 is simplified to Eq. 3.8 due to Ampère's law. This, however, does not take the diameter of the coil into account. The diameter of the coil will affect the Faraday rotation per unit length, $f$, according to

$$f \propto \frac{I}{\lambda^2 D} \tag{4.3}$$

where $\lambda$ is the wavelength of operation and $D$ is the diameter of the coil [6]. This shows a larger Faraday rotation for smaller diameter. However, smaller diameter will result in more stress on the fiber and causes a more

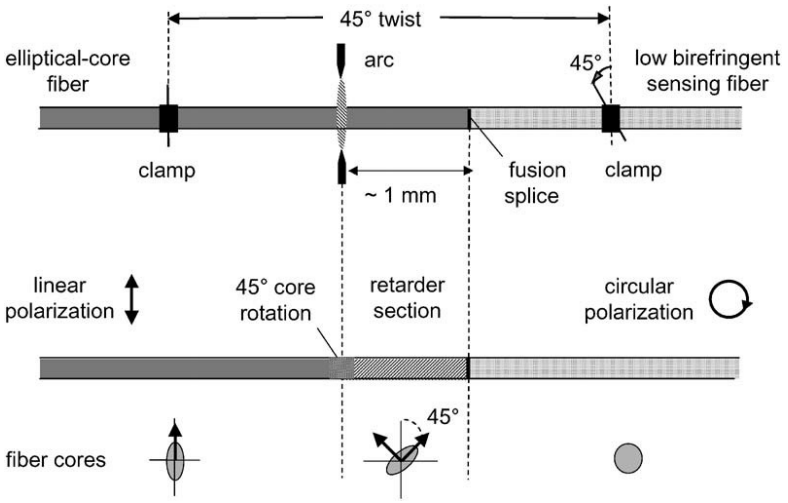


Figure 4.4: The principle of creating a quarter-wave phase retarder by fusing elliptical-core fiber and low birefringent fiber together [5].

bend-induced linear birefringence. This will deteriorate the sensitivity of the sensor unless it is suppressed and at the same time keep the coil sensitive to the Faraday effect. Twisting the fiber will induce a circular birefringence as mentioned in section 3.1. If the induced circular birefringence dominates linear birefringence may be neglected. Circular birefringence will rotate the polarization but will preserve the polarization state [11]. However, if twisted too much the fiber may be broken so there is an upper limit to what degree the fiber can be twisted. When manufacturing small sensing coils this can be a problem. As mentioned before, small coils will have more linear birefringence and therefore the twist rate also has to be larger and may exceed the upper twist limit. Laming and Payne [6] found that the minimum coil size with twisted fiber is around 20 cm in diameter.

To overcome the above problem a more sophisticated technique can be used. Instead of twisting the fiber after manufacturing they can be spun during the fiber drawing process. A spun fiber can viewed as a fiber with an ideal cross-section and is referred to spun low-birefringent (LowBi) fiber [6]. Nevertheless, the limitations of the sensing coil radius still remains. To overcome this spun highly birefringent (SHB) fiber can be used instead. This type of fiber is fabricated by using PM fiber instead of standard fiber during the drawing process. SHB have very little residual birefringence and is almost immune to bend-induced linear birefringence and therefore this fiber type can be used in small multiturn sensing coils while keeping the sensitivity. This will enable measurement in the submilliamp region [6]. Despite the ability to cancel out linear birefringence there is still the issue of thermally induced-

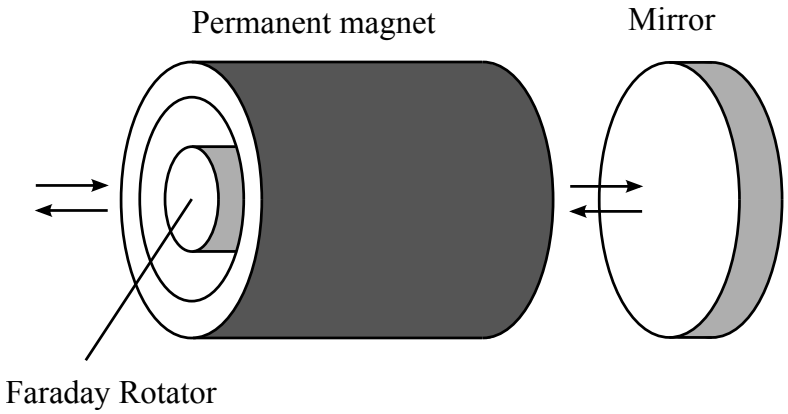


Figure 4.5: A Faraday Mirror. The wave enters the Faraday rotator and the polarization is rotated 45° due to the Faraday effect. Then the wave is reflected and once again rotated 45° which results in a total rotation of 90°.

stress which results in a temperature dependence.

### 4.3.4 Mirror in the reflection configuration

In the previous section spun fibers were mentioned as an approach to cancel out the undesirable linear birefringence in the sensing coil. Laming and Payne [6] mention yet another approach in order to cancel the linear birefringence. This approach is to conjugate the orthogonal components to exploit the reciprocity of the linear birefringence. This is done by placing an orthoconjugate retroreflector (OCR), better known as Faraday mirror (FM), at the end of the sensing coil which will rotate the polarization state with an angle of 90°. This will result in a wave propagating back through the sensing coil with the orthogonal components swapped compared to a wave in the forward direction, i.e. the component that is right-hand circularly polarized in the forward direction will become left-hand circularly polarized after reflection and vice verse. The phase shift for the different components will be equalized and in the ideal case the effect of linear birefringence will disappear. The reflection configuration described in Section 4.1 utilizes a Faraday mirror.

A Faraday mirror consists of a Faraday rotator placed inside a permanent magnet and a mirror, as shown in Fig. 4.5. The wave enters the rotator and experiences a 45° rotation, reflected in the mirror and experiences another 45° rotation due to the non-reciprocity of the Faraday effect. Recall that the Verdet constant is wavelength dependent so Faraday mirrors are specified for a certain wavelength and will not achieve 90° rotation for other wavelengths. A schematic of a Faraday mirror is shown in Fig. 4.5. An experminent per-

formed by Laming and Payne [6] showed that the sensitivity of the reflection configuration without a Faraday mirror, using an aluminum mirror instead, had a variation of ±25 % when the temperature was increased from 20°C to 70°C. With a Faraday mirror the variation of the sensitivity was only ±2 %. This variation in sensitivity is a result of temperature dependent linear birefringence. Although it provides a good compensation a Faraday mirror is bulky and requires shielding from magnetic fields.

Another experiment performed by Pistoni et.al. [19] also compares the performance with and without a Faraday mirror but is focused on mechanical vibrations instead. The setup includes a 5 loop sensing coil around a conductor with a 50 A rms AC with a frequence of 50 Hz. The measurement with a normal mirror had a noise level of two orders of magnitude higher then the measurement with a Faraday mirror.

# Chapter 5

# Measurements

In order to increase the sensitivity of the fiber optic current sensor, the Faraday effect (induced circular birefringence) must overcome the linear birefringence. For the measurements in this thesis a Faraday mirror will be used in order to try to suppress the induced linear birefringence. A polarimeter samples the normalized Stokes parameters with 1000 points for all measurements. A 1000 meter long SMF will be used as the sensing coil.

## 5.1 Method for optimizing the Faraday mirror

The first step is to find the optimal wavelength of operation for the Faraday mirror. The centre wavelength of this Faraday mirror is 1550 nm $\pm$ 15 nm. A polarization scrambler is used to scramble the polarization by inducing linear birefringence. Using the standard deviation for the Stokes parameters and measuring on several wavelengths the most suited wavelength for the Faraday mirror can be determined. The wavelength for which the standard deviation is the smallest will be chosen as operation wavelength. The setup for the wavelength optimization is shown in Fig. 5.1. The "scrambler" consists of 2 quarter-wave plates and 2 half-wave plates, which are controlled by 2 signal generators. Before performing measurement with the Faraday mirror just the scrambler is connected directly to the polarimeter. Using the signal generators, different frequencies and amplitudes of the voltage are used in order to achieve as uniform coverage as possible of the Poincaré sphere. For a uniformly covered sphere the standard deviation is 0.5 for each Stokes parameter.

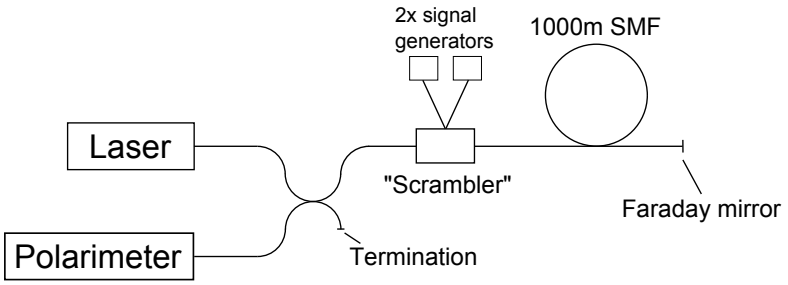


Figure 5.1: Setup in order to determine the center wavelength for the Faraday mirror.

## 5.2 Method for current measurements

When the center wavelength of the Faraday mirror is determined current measurements can be performed. Current measurements were performed up to 1000 A with three different polarization states. The setup for the current measurements is almost the same as during the wavelength optimization but without the scrambler. The setup is shown in Fig. 5.2. The measurements are done by sampling the Stokes parameters for currents from 0 A to 1000 A with a step size of 100 A. In order to calculate the measured current the angle of the polarization ellipse is calculated using

$$\theta = \frac{1}{2}\arctan\left(\frac{\overline{S_2}}{\overline{S_1}}\right) \tag{5.1}$$

for each current level using the mean value for the Stokes parameters. Then the current is calculated by first calculating the angle of rotation for each current level according to

$$\Delta\theta_I = \theta_I - \theta_{Zero} \tag{5.2}$$

and the using equation (3.7) which gives

$$I = \frac{\theta}{2VN} \tag{5.3}$$

where the factor 2 in the denominator is due the fact that in this case the light will experience the Faraday effect twice since it propagates both back and forth in the sensing coil. The number of turns is $N \approx 2100$. The current will also be measured using zero flux technique in order to obtain a reference value.

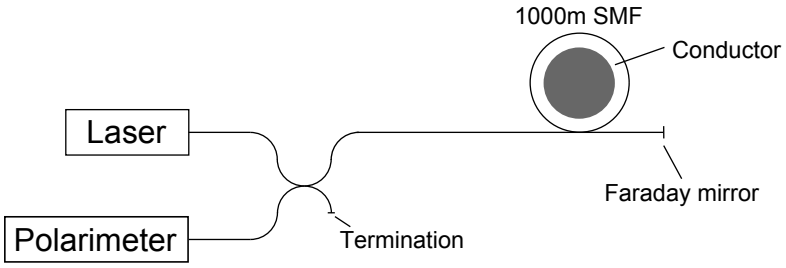


Figure 5.2: Setup for the current measurements.

# Chapter 6

# Results

## 6.1 Wavelength optimization

The wavelength optimization was performed at three different times in order to see if the results are repeatable. In Fig. 6.1 and Fig. 6.2 standard deviation for all Stokes parameters for wavelengths between 1500 nm and 1600 nm and between 1545 and 1555 nm, respectively. The second and third measurements have similarities but differs a lot from the first measurement. At the point where the standard deviation is the smallest is should be at the wavelength were the Faraday mirror has 90° rotation and hence it is reasonable to assume that the standard deviation will decrease until it reaches that wavelength and then increase again. Both Fig. 6.1b and Fig. 6.1c have the desired look whereas Fig. 6.1a looks strange. Looking at the smaller interval in Fig. 6.2 the first measurement also looks strange and second and third measurement have the same look and hints that the most suited wavelength is slightly above 1555 nm. In Fig. 6.3a a fourth and final wavelength optimization measurement are performed and with an expanded interval around 1550 nm. Using the same way of thinking as before, this plot also has a desired look and the most suited wavelength is around 1560 nm wavelength. Adding the standard deviation of all three parameters the plot looks like Fig. 6.3b and the optimal wavelength can be chosen to 1559 nm.

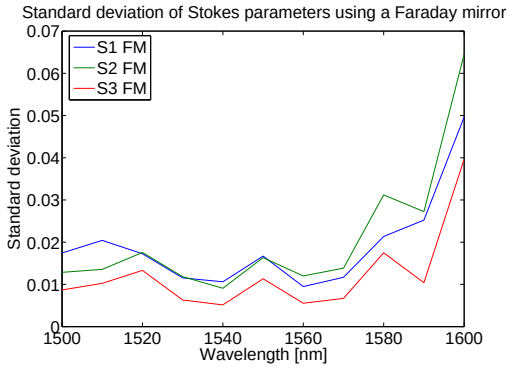


(a)

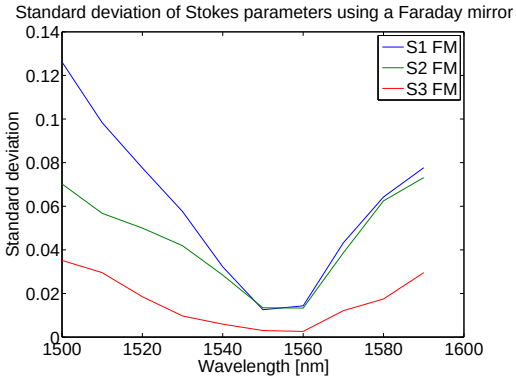


(b)

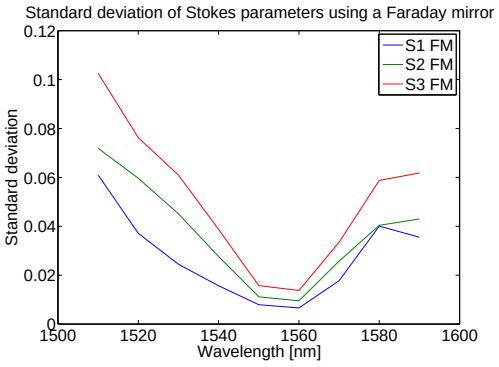


(c)

Figure 6.1: Standard deviation for all Stokes parameters for wavlengths between 1500 nm and 1600 nm at three different times.

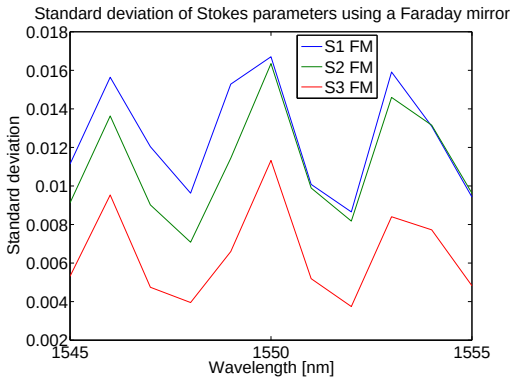


(a)

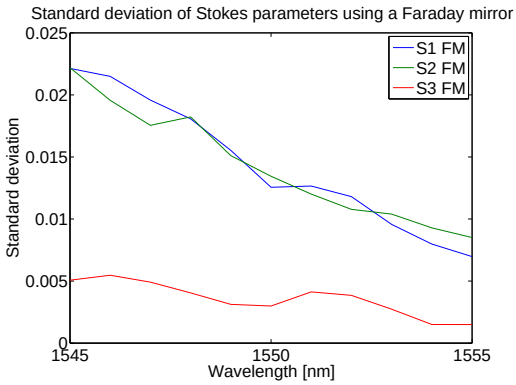


(b)

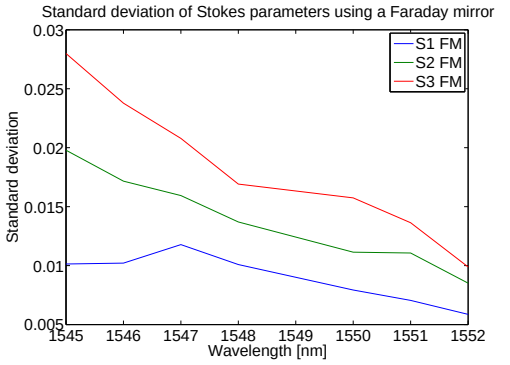


(c)

Figure 6.2: Standard deviation for all Stokes parameters for wavlengths between 1545 nm and 1555 nm at three different times.

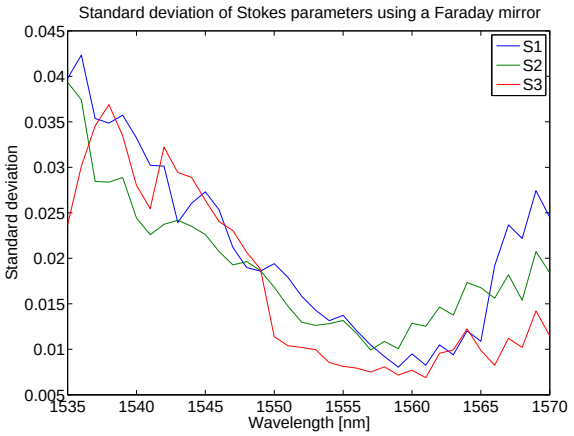


(a)

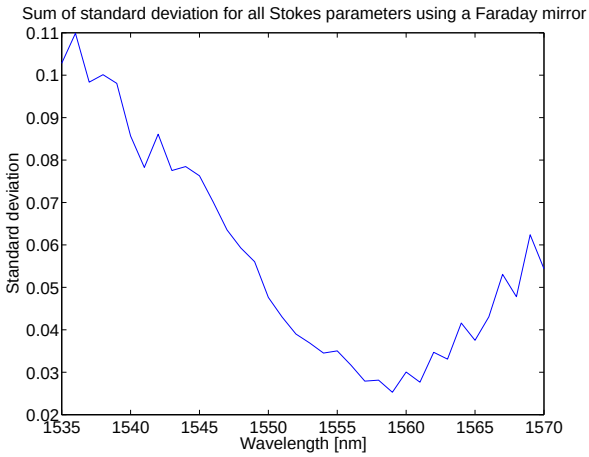


(b)

Figure 6.3: Standard devation for all three Stokes parameters for wavelengths between 1535 nm and 1570 nm and the sum of all standard deviations.

## 6.2 Current measurements

### 6.2.1 Static current

As mentioned previously, the most suited wavelength for the Faraday mirror is 1559 nm. For this wavelength the Verdet constant is $V = 0.733\ \mu\text{rad} \cdot \text{A}^{-1}$. The first current measurements for three different polarizations are shown in Fig. 6.4. The first polarization is linear, the second polarization is elliptical and the third is almost circular. Another current measurement were performed but for only two different polarization states. The result is shown in Fig. 6.5. The first polarization is linear and the second is elliptical. In both measurements a relatively good linearity can be observed with a few exceptions. In order compare the two different types of measurements the ratio between these are plotted in Fig. 6.6. Disregarding the ratio for 100 A for the first polarization, the ratio for both first and second polarization are almost kept within 10 and 12 for all current levels. It can also be noticed that the ratio for these two polarizations are similiar.

In order to analyze this further, the normalized Stokes parameters are plotted in Fig. 6.7. One undesired effect that can be observed is that the fourth Stokes parameter, $S_3$, is changing with the current level. In some sense this can be construed as induced linear birefringence, i.e. the magnetic field from the conductor not only causing rotation of the plane of polarization but also transform the polarization to either more circular or less circular. One other oberservation is that in the first polarization state, Fig. 6.7a, $S_3$ first decreases but then starts to increase.

To summarize these observations, the output polarization is not entirely stable. Nor is this configuration very sensitive to the Faraday Effect. This may depend on the fact that the wave is affected by both linear birefringence and the Faraday effect simultaneously and along the whole sensing fiber. These effects need to be considered as distributed along the whole sensing fiber. Whereas the Faraday effect tries to rotate the plane of polarization, the linear birefringence in the sensing fiber is transforming the polarization back and forth through different states of polarization, causing significantly degradation of the sensitivity of the sensing coil. It should also be noted that the polarzation is monitored after back propagation through the whole sensor, and this polarization is not necessarily the same as the polarization at the input of the sensing coil.

### 6.2.2 Current sweep

Measurements on changing current during the sampling sequence were also performed. This is shown in Fig. 6.8. In Fig. 6.8a the current is swept from 0 A to 1000 A and in Fig. 6.8b the current is swept from 1000 A to 0 A. During the first sweep the fiber between the sensing coil and the coupler are parallel with the conductor and during the second sweep the same fiber part are perpendicular to the conductor. The reason for doing these measurements is that when this specific fiber part changed the polarization drastically. This is part of the sensor where we have both back and forward propagating waves and that the polarization is affected this much is undesirable.

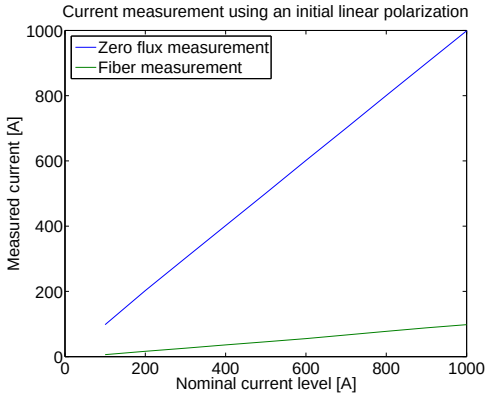


(a)

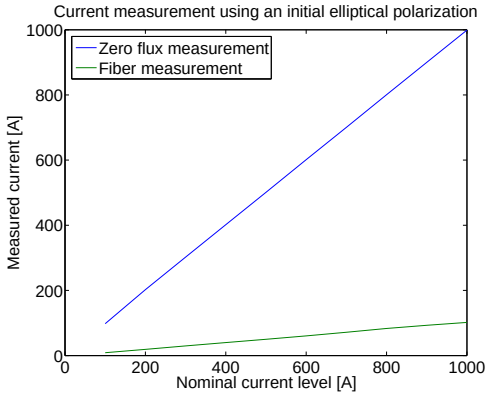


(b)

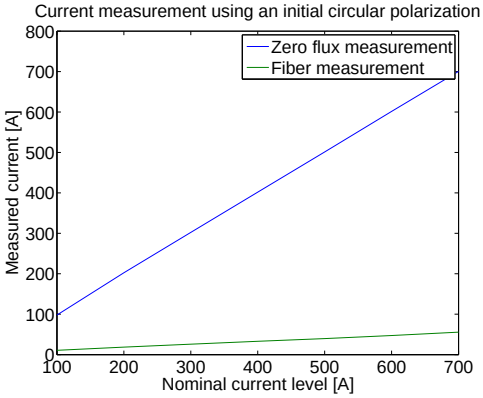


(c)

Figure 6.4: First current measurement on three different polarizations.

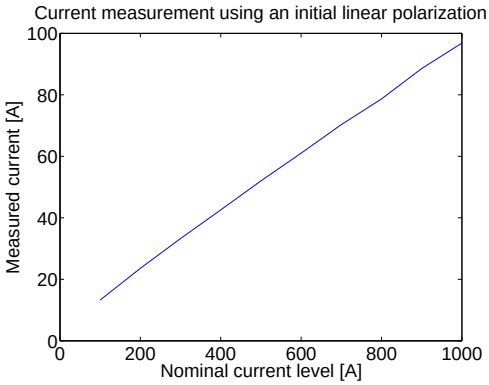


(a)

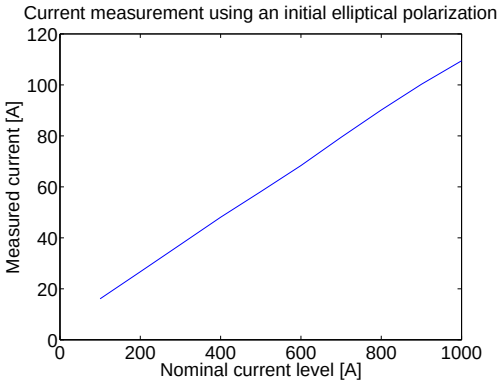


(b)

Figure 6.5: Second current measurement on two different polarizations.

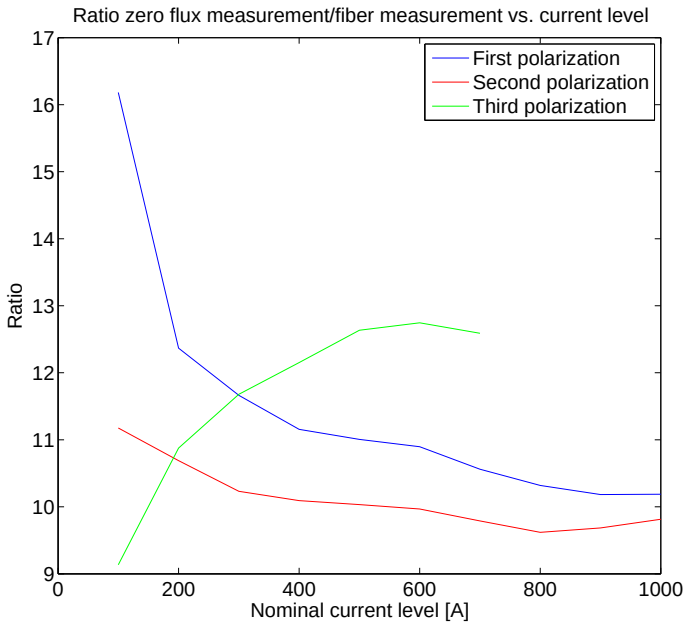


Figure 6.6: The ratio between the value of the zero flux measurement and the value of the fiber measurement at three different polarizations.

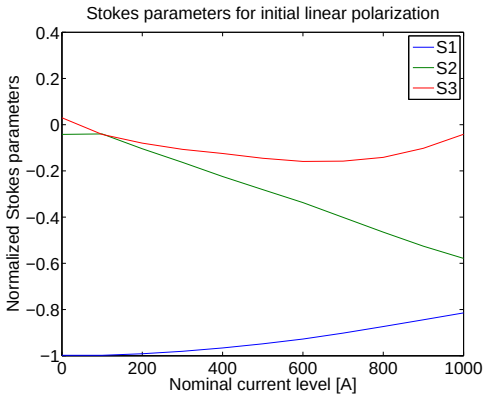


(a)

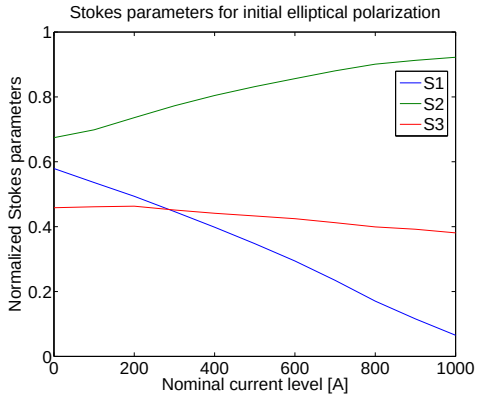


(b)

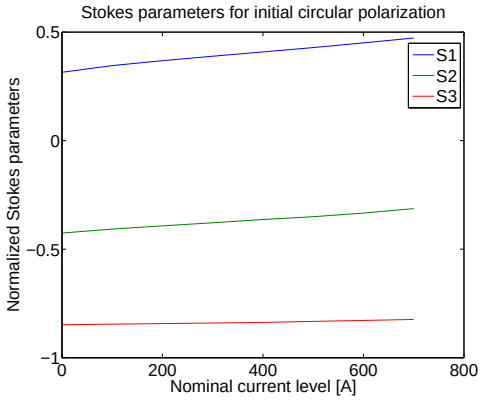


(c)

Figure 6.7: Stokes parameters for the different polarizations.

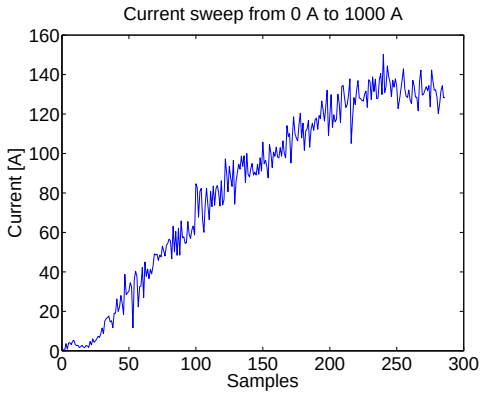


(a)

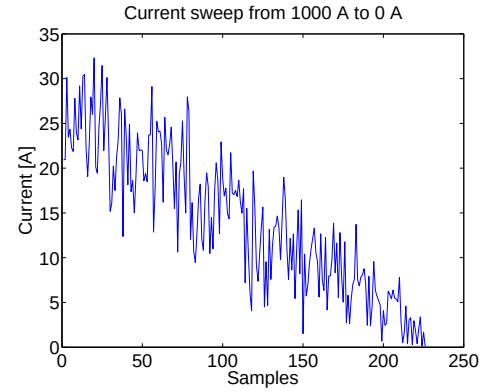


(b)

Figure 6.8: Current measurement on current sweep. In the first figure the current is swept from 0 A to 1000 A and in the second figure the current is swept from 1000 A to 0 A.

# Chapter 7

# Conclusion

In this project the foundations of fiber optic current sensors have been explored. There are several different configurations in order to detect the Faraday effect, where the Sagnac configuration and the In-line reflection configuration are the most common. From the literature it can be concluded that the reflection configuration seems more promising then the Sagnac configuration because of the insensitivity to mechanical disturbance.

Even though there are several advantages for these types of sensors compared to conventional current measurements methods, there are still the matters of undesirable effects such as induced linear birefringence which will decrease the sensitivity of the sensor

Another consideration is the Verdet constant. For silica fiber the Faraday effect is relatively weak which will require either a very accuratly signal processing unit or a large number of loops in the sensing coil in order to detect the Faraday effect for low current levels. A large number of loops will induce even more linear birefringence.

Several techniques can be used in order to cancel the undesirable linear birefringence such as using a Faraday mirror and using specially manufactured fibers. From the measurements in this project it is reasonable to assume that with a large number of loops in the sensing coil the Faraday mirror alone is not enough. Although, SMF may achieve sufficient sensitivity in large single loop coils.

One must also be aware of the occurence of wrap around. If multiturn coils are used around conductors with high current, this can result in a Faraday rotation larger than $2\pi$ and the signal may be interpreted as much lower than it actually is. This can be solved by either a more sophisticated signal processing unit or using different coils for different current levels.

The Verdet constant will decrease with increased wavelength and the wavelength used in the measurements in this project is not preferable, shorter

wavelength should be used. Using shorter wavelengths will decrease the required number of turns which in turn will result in less linear birefringence.

In this project the source and the signal processing unit has not been investigated. Although it has been concluded in previous work that a low coherent source can eliminate undesirable effects due to polarization cross coupling, this may be a good idea to investigate more thorougly in future work.

# Bibliography


[1] Tesla vs. Edison: the war of the currents `http://www.abb.com/cawp/seitp202/c646c16ae1512f8ec1257934004fa545.aspx` 2014-04-30

[2] G.Frosio and R.Dändliker, "Reciprocal reflection interferometer for a fiber-optic Farady current sensor", *Appl. Opt.*, vol. 33, no. 25, pp. 6111–6122, Sep. 1994.

[3] K.Bohnert, P.Gabus, J.Nehring and H.Brändle, "Temperature and vibration insensitive fiber-optic current sensor", *J. Lightw. Technol.*, vol. 20, no. 2, pp. 267–276, Feb. 2002.

[4] N.Peng, Y.Huang, S.Wang, T.Wen, W.Liu, Q.Zuo and L.Wang, "Fiber optic current sensor based on special spun highly birefringent fiber", *IEEE Photon. Tech. Letters*, vol. 25, No. 17, pp. 1668–1671 Sept. 2013

[5] K. Bohnert, P.Gabus, J.Kostovic, H.Brändle, "Optical fiber sensors for the electric power industry", *Opt. Eng.*, vol. 43, pp.511–526, July 2004.

[6] R.I.Laming and D.N.Payne, "Electric current sensors employing spun highly briefringent optical fibers", *J. Lightw. Technol.*, vol. 7, no. 12, pp. 2084-2094, Dec. 1989.

[7] A.H.Rose, S.M.Etzel and C.M.Wang, "Verdet constant dispersion in annealed optical fiber current sensors", *J. Lightw. Technol.*, vol. 15, no. 5, pp. 803–807, May 1997.

[8] E.Hecht, *Optics*, 4th ed. Addison Wesley, 2002.

[9] L.Lundberg, "An In-band OSNR monitoring method for polarization multiplexed QPSK signals using Stokes parameters", Master thesis in photonics engineering, Chalmers University of Technology, 2013.

[10] A.G.Santos et. al., "Polarization ellipse and Stokes parameters in geometric algebra", *J. Opt. Soc. Am. A*, vol. 29, no. 1, pp. 89-98, Jan. 2012.

[11] Recent progress in optical fiber research, Edited by Moh. Yasin, Sulaiman W. Harun and Hamzah Arof, ISBN 978-953-307-823-6, 462 pages, Publisher: InTech, Chapters published January 25, 2012 under CC BY 3.0 license

[12] B.Lee, "Review of the present status of optical fiber sensors", *Opt. Fiber Tech.*, vol. 9, no. 2, pp. 57–79, 2003

[13] S.Donati, V.Annovazzi-Lodi, T.Tambosso, "Magneto-optical fibre sensors for electrical industry: analysis of performances", *IEE Procedings*, vol. 135, No. 5,pp. 372–382, Oct. 1988

[14] P.Drexler and P.Fiala, "Utilization of Faraday Mirror in fiber optic current sensors", *Rad. Eng.*, vol. 17, no. 4, pp. 101–107, Dec. 2008.

[15] Faraday effect, Wikipedia, `http://en.wikipedia.org/wiki/Faraday_rotator` 2013-09-11

[16] M.Takahashi, K.Sasaki, A.Ohno, Y.Hirata and K.Terai, "Sagnac interferometer-type fibre-optic current sensor using single-mode fibre down leads", *Meas. Sci. Technol.*, vol 15, pp.1637–1641, 2004

[17] P.A.Willams,A.H.Rose,G.W.Day,T.E.Milner and M.N.Deeter, "Temperature dependence of the Verdet constant in several diamagnetic glasses", *Appl. Opt.*, vol. 30, no. 10, April 1991.

[18] J.Blake, P.Tantaswandi, R.T.de Carvalho, "In-line Sagnac interferometer current sensor", *IEEE Transactions on Power Delivery*, vol. 11, no. 1,pp.116–120, Jan. 1996

[19] N.C.Pistoni and M.Martinelli, "Vibration-insensitive fiber-optic current sensor", *Opt. Lett.*, vol. 18, no. 4, pp. 314–316, 1993